Theoretical Treatment of the Thermophysical Properties of Fluids Containing Chain-like Molecules

Final Report for the period June 1, 2003-May 31, 2006
Submitted to the Department of Energy
Contract Number DE FG02-97ER14771

Carol K. Hall

ABSTRACT

This research program was designed to enhance our understanding of the behavior of fluids and fluid mixtures containing chain-like molecules. The original objective was to explain and predict the experimentally observed thermophysical properties, including phase equilibria and dynamics, of systems containing long flexible molecules ranging in length from alkanes to polymers. Over the years the objectives were expanded to include the treatment of molecules that were not chain-like. Molecular dynamics and Monte Carlo computer simulations were used to investigate how variations in molecular size, shape and architecture influence the types of phase equilibria, thermodynamic properties, structure and surface interactions that are observed experimentally. The molecular insights and theories resulting from this program could eventually serve as the foundation upon which to build correlations of the properties of fluids that are both directly and indirectly related to the Nation's energy resources including: petroleum, natural gas, and polymer solutions, melts, blends, and materials.

Introduction

The major projects conducted under DOE sponsorship in the project period were: (1) Gibbs-Duhem Monte Carlo simulation of complete phase diagrams for binary mixtures, (2) phase behavior and structure of block-copolymer nanocomposites, (3) computational design of pattern recognition surfaces, (4) lattice Monte Carlo simulation of DNA hybridization on microarrays, (5) modeling of the formation of mechanically-assisted monolayers, and (6) computational exploration of the self assembly of dipolar colloidal particles to facilitate the design of smart materials . Below we describe the highlights of our accomplishments in each of these projects over the report period. A list in chronological order of publications resulting from this grant over the reporting period is given at the end of this report. Citations appearing in the description below are taken from that list.

(1) Gibbs Duhem Monte Carlo Simulation of Complete Phase Diagrams for Binary Mixtures

The classical work of Scott and Van Konynenberg on the classification of the dependence of the types of binary mixture phase diagrams observed on molecular energetics parameters was extended to include the solid phase. This was achieved by performing Gibbs-Duhem Monte Carlo computer simulations of complete (i.e. containing solid, liquid and vapor) phase diagrams for binary mixtures of Lennard Jones fluids at a variety of points in the space spanned by the interaction parameters. [1] [3, 4] It was found that for mixtures in which the components have greatly dissimilar critical temperatures, the presence of the solid phase significantly alters the fluid phase equilibria. In those cases, the phase behavior classification based on experimental observations differs significantly from that predicted by an equation-of-state approach.

The Gibbs Duhem integration technique was then extended to calculate ternary phase diagrams, with particular focus on solid–fluid phase equilibria, for mixtures of Leonard Jones molecules at constant temperature and pressure. [17] The simulation parameters were selected to roughly model a mixture of two diastereomeric molecules with similar melting points and molecular diameters immersed in a solvent with a lower melting point and a slightly smaller diameter. Ternary phase diagrams for an equimolar mixture of the diastereomers were determined at a series of temperatures. We found a range of temperature and solvent concentrations at which only one of the diastereomers precipitated, thus effecting a separation of the diastereomers. These results are applicable to classical resolution, a separations method in which the two race mates in a racemic mixture are reacted with a resolving agent to form two diastereomers, which can then be separated because they have different physical properties. A sample phase diagram illustrating this point is shown in Figure 1. Our results show that: (1) there exists a range of solvent concentrations at which an equimolar mixture of diastereomers separates into a liquid and a solid rich in one of the two components, and (2) this equilibrium shifts from one component to the other as the temperature increases. It is for this range of solvent concentration that separation of diastereomers is possible.

We next investigated the phase behavior of systems containing diatomic molecules modeled as Lennard Jones dumbbells. We began by calculating vapor-liquid phase diagrams for single-component and binary-mixture Lennard-Jones dumbbell systems using the Gibbs-Duhem integration method. [10] Our results were compared to experimental data on simple non-spherical molecules such as O_2, N_2, C_2H_6 and CO_2 .We also investigated the effect of varying well-depth ratios on the phase behavior.

Finally we calculated solid-liquid phase diagrams for single-component and binary mixtures of Lennard-Jones dumbbell molecules. [12] We began by calculating the equation of state for pure fluids containing C_2H_6, CO_2 and F_2, all of which were modeled as linear diatomic molecules interacting via a two-center Lennard Jones potential. The Frenkel-Ladd thermodynamic interaction method was used to calculate the free energies of each phase. The equations of state and free energies were then used to obtain solid-liquid coexistence points for the pure fluids. These, in turn, were used as initial conditions in Gibb-Duhem integration calculations of phase diagrams for model binary mixtures of Lennard Jones dumbbell fluids. The effects of molecular size and attractions on the solid-liquid phase diagrams were explored.

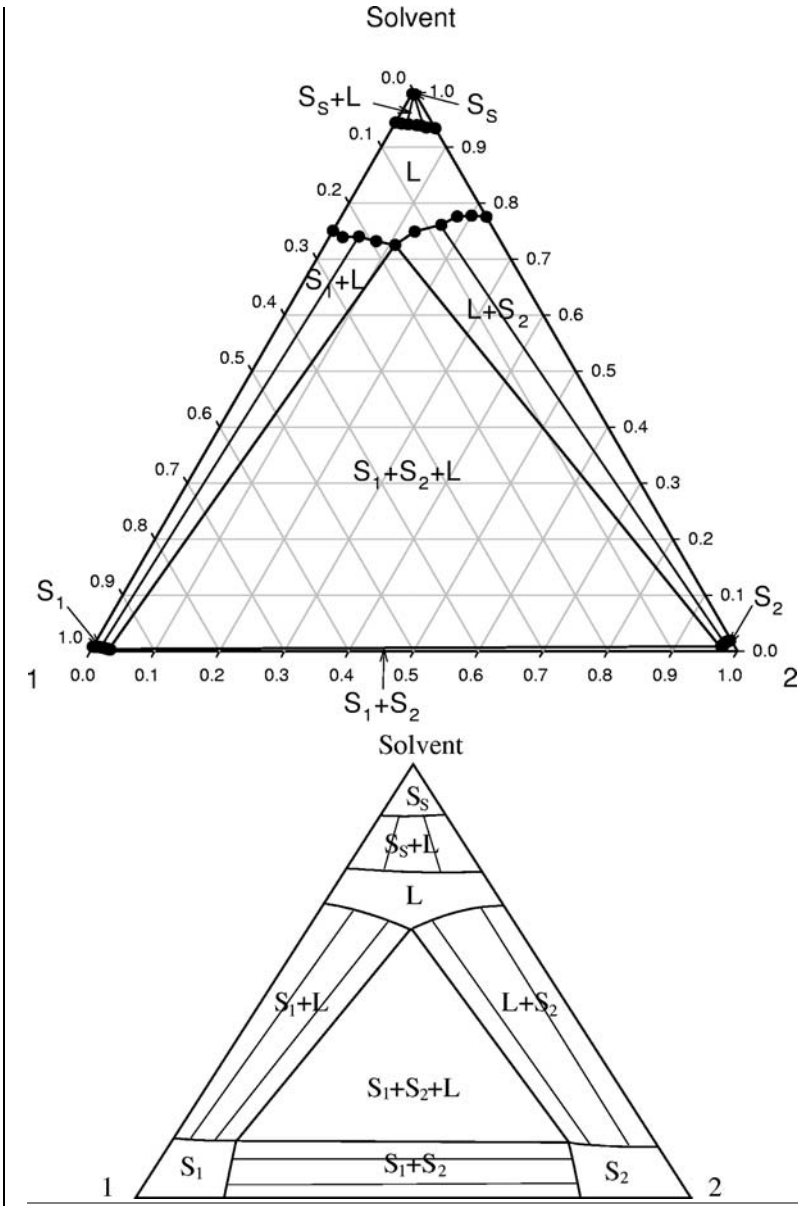

Figure 1: Ternary phase diagram calculated at $T^* = 0.67$, $P^* = 0.040$ and $\varepsilon_{12} = 1.822$, $\sigma_{12} = 1.163$. The upper graph is data calculated by the Gibbs Duhem integration technique and the bottom graph is a schematic of the upper graph. Mixtures with an equal concentration of the diastereomers (components 1 and 2) and a solvent mole fraction between 0.69 and 0.75 will separate into a solid phase rich in component 2 and a liquid phase. [17]

(2) Phase Behavior and Structure of Block-copolymer Nanocomposites

Block copolymers continue to be great interest for many reasons, one of which is that they exhibit unique phase behavior on the nanoscale. Block copolymers form structures that have a number of unusual properties including well-defined domain size, long-range ordering, and mechanical and optical anisotropy. Once an ordered copolymer structure has been formed, it can be used as a matrix within which to order another species, such as nanoparticles. The resulting composite material combines the attractive technological features of both constituents. The variety of block copolymer morphologies and nanoparticles available yields a multitude of possible applications including high-density information storage media, magnetic fluids, medical diagnostics, molecular semiconductors, selective membranes, lithium batteries, catalysts, etc

We used discontinuous molecular dynamics simulation to study the phase behavior of diblock copolymer/nanoparticle composites. [2, 6] The copolymers were modeled as chains of tangent hard spheres with square-shoulder repulsions between unlike species; the nanoparticles were modeled as hard spheres with square shoulder repulsion with one of the copolymer blocks. Phase diagrams for the copolymer- nanoparticle systems in the $\chi_{AB}N$ vs. Φ_P plane were calculated for composites contain nanoparticles of various diameters and interaction strengths. These are shown in Figure 2. Here χ is the effective interaction strength (the Flory chi parameter) between copolymer components, N is the chain length and Φ_P is the volume fraction of nanoparticles). These diagrams exhibited a rich behavior, showing lamellae, perforated lamellae, cylinders and disordered phases. Two-phase coexistence between different copolymer phases or between a copolymer phase and a nanoparticle (depending upon the nanoparticle interaction strength) was also found for composites containing large nanoparticles.

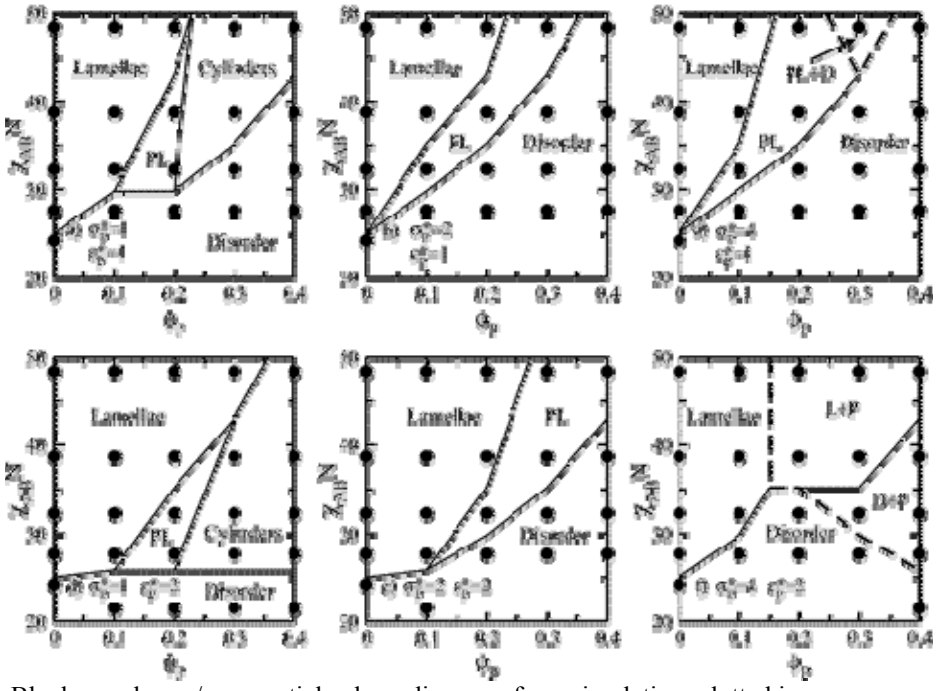

Figure 2. Block copolymer/nanoparticle phase diagrams from simulation, plotted in $\chi_{AB}N$ vs Φ_P space for particle diameters= 1, 2, and 4 (columns 1, 2, and 3) and particle-segment interactions = 1 and 2 (rows 1 and 2). [6]

We also calculated the concentration profiles perpendicular to the lamellar interface for nanoparticles of different sizes and interaction strengths. As expected, neutral nanoparticles concentrate at the interface between copolymer domains while interacting nanoparticles

concentrate within the favorable domain. The larger nanoparticles were more easily localized, but had less impact on the copolymer concentration profiles. The locations of the phase transitions were in qualitative agreement with theoretical predictions, but the concentration profiles were inconsistent with theoretical predictions. The variation of the spacing with nanoparticle volume fraction was consistent with experimental data.

Finally, we developed a new method for extracting concentration profiles from molecular simulation data based on direct analysis of the structure factor, S(q), thus avoiding the commonly-encountered ambiguities associated with fitting data to hypothetical model geometries.[11]

(3) Computational Design of Pattern Recognition Surfaces (joint project with Professor Jan Genzer)

Interest in the adsorption of heteropolymers at chemically heterogeneous surfaces emanates from numerous scientific applications of heteropolymer adsorption on heterogeneous surfaces such as adhesion, chromatography, nanoscale patterning and masking, and biomedical implant modification. Theoretical research to date in this area has focused primarily on understanding the mechanism of adsorption of copolymers (block, alternating, and random copolymers) onto substrates with fixed chemical patterns. We adopted a different approach. Instead of fixing the surface pattern and assessing the sequence statistics of the copolymers that bind to it, we fixed the copolymer sequence statistics and found a surface pattern that optimizes copolymer adsorption for a given monomer sequence through the use of lattice Monte Carlo simulation. [7, 9]

Specifically, we considered a system of AB copolymers of length 24 with varying sequence distribution: $(AB)_{12}$, $(A_2B_2)_6$, $(A_3B_3)_4$, $(A_4B_4)_3$, $(A_6B_6)_2$, and $(A_{12}B_{12})_1$ adsorbed on a surface containing two types of sites: 1 and 2, with 1 sites preferring A segments and 2 sites preferring B segments. By performing identity switch moves on two randomly-picked surface sites, the surface evolved towards an optimal surface pattern that could recognize and selectively absorb the sequence in the copolymer. For copolymers with less blocky sequences, the designed surfaces recognize and selectively absorb the correct sequences when the surface segment interactions dominate the intersegment attractions. For copolymers with more blocky sequences, recognition is good when the segment–surface interactions are only slightly stronger than the intersegment interactions. Figure 3 show examples of the surface "designed" to adsorb each of the six types of copolymers.

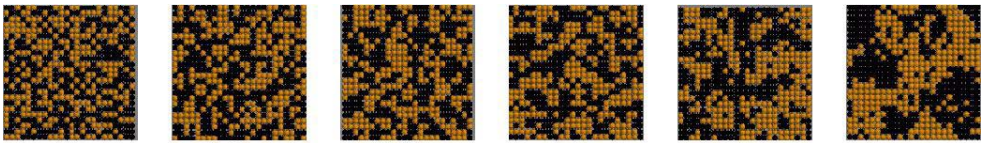

Figure 3: Surfaces designed to recognize the respective sequence.[7]

Our design method should prove useful in exploring the relationship between the spatial distribution of chemical heterogeneities in biopolymers and heterogeneities on an adsorbing surface, and thus contribute to current understanding of transmembrane signaling, pathogen-host interactions, viral inhibition, etc.

(4) Lattice Monte Carlo Simulation of DNA Hybridization on Microarrays (joint project with Professor Jan Genzer)

We decided to extend the pattern recognition work described above to an interesting application—namely the hybridization of DNA on microarray slides. A microarray is a small glass or nylon slide containing thousands of single-stranded genes or gene fragments immobilized on the surface in spots arranged in a grid, with one gene represented per spot. Fluorescently labeled single–stranded "target" genes in a sample solution exposed to the microarray surface bind specifically ("hybridize") to complementary immobilized "probe" DNA molecules on the microarray surface. The objective of this work was to obtain a broad physical picture of molecular recognition in DNA microarrays and to develop a set of general guidelines for maximizing microarray sensitivity and specificity.

The probe molecules and target molecules were modeled as self-avoiding chains on a cubic lattice. [13] Each of the segments along the probe molecule recognized (preferentially attracts) and bound uniquely to its complementary segment on the target with an attractive hybridization energy ε, in order to mimic the complementary nucleotide pairs (A-T, G-C) on DNA. The probe and target molecules considered in our simulations are such that the i^{th} segment on the probe is complementary only to the j^{th} segment on the target, the $i+1^{th}$ segment on the probe is complementary only to the $j+1^{th}$ segment on the target, and so on.. A cartoon of the hybridization, where the blue chain represents the probe and the red chain represents the target. are shown below.

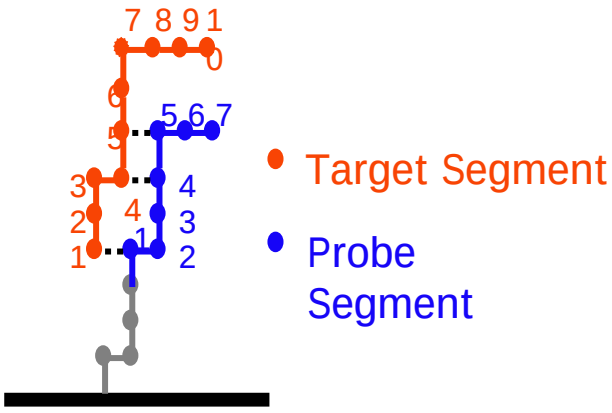

Figure 4: Cartoon showing the hybridization of a lattice target DNA molecular onto a lattice probe DNA molecule. [13, 15, 16]

Lattice Monte Carlo simulations were performed on systems containing multiple freely-floating target molecules and multiple probe molecules tethered to a hard surface. [16] The target molecule contained 48 statistical segments and the probe molecules contained 8 to 24 segments. We examined how the hybridization of the probe and the target was affected by increasing the surface density of the probes (the number of probe molecules per unit surface area) and increasing the target concentration (the number of target molecules in solution).

Highlights of our simulation results are the following. As the surface density increased, the lack of space in the lateral (x-y) direction made the probes stretch out and extend in the z direction. For longer probes as the surface density increased, the probability of binding long stretches of target segments (specificity) decreased and the probability of binding short stretches increased. For shorter probes (8 and 12 segments) there was an optimum surface density which provided the highest probability of binding all probe segments to the target (specificity). The data in Figure 5 suggests an optimum surface density between 0.0000694 and 0.00278 molecules per

nm^2 while typical surface densities in microarrays lie in the range 0.00012 – 0.4 probe molecules per nm^2 surface area [6, 7]. Our optimal density is towards the lower end of this range. For all probe lengths, as the surface density increased, the target was less likely to bind completely to one probe, and instead bound simultaneously to more than one probe, making it harder to detect a mismatch.

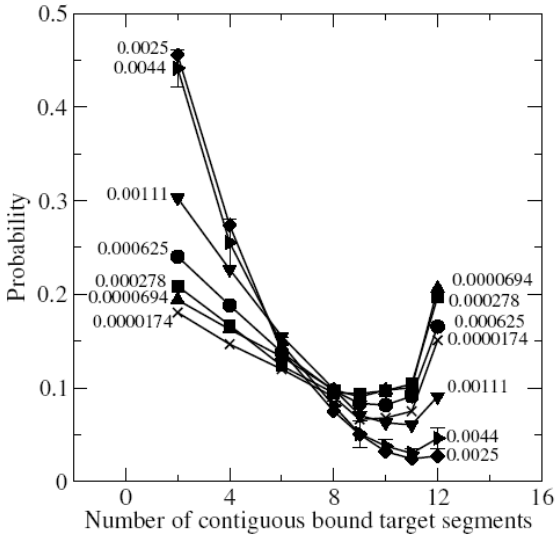

Figure 5. Probability of a contiguous stretch of segments along target binding to segments along end type probes of length 12 segments at $\varepsilon = 3kT$ for 0.0000174 (cross), 0.0000694 (triangle), 0.000278 (square), 0.000625 (circle), 0.00111 (inverted triangle), 0.0025 (diamond), and 0.0044 (right triangle) probes molecules per nm2 surface area. [16]

We also studied the kinetics of hybridization propagation. [15] We used theory to derive a mathematical expression for a time correlation function c(l; t) that provides insight into the zipping phenomena along any type of polymer, including DNA, undergoing a conformational transition. For DNA hybridization, the conformational transition is the binding together of target and probe to form a double helix. The polymer was modeled as an Ising-like chain with each segment being in one of two states: bound (+1) or unbound (-1). The time correlation function c(l; t) predicts the correlation between the state of the j^{th} segment at time 0 and the state of the $j \pm l^{th}$ segment at time t. The results obtained so far can serve as a first step towards developing a more comprehensive theory capable of accurately describing DNA hybridization.

(6) Computational Exploration of the Self-assembly of Dipolar Particles to Facilitate the Design of "Smart" Materials (joint project with Professor Orlin Velev)

Colloid particles containing asymmetric or dipolar charge distribution self assemble into a variety of interesting microstructures such as nematic or smectic liquid crystals, co-crystals of novel symmetry (in mixtures of different size particles) and open networks (gels) containing long chains of particles. Our collaborator, Professor Orlin Velev of the NCSU Department of Chemical and Biomolecular Engineering knows how to make such particles in his laboratory. The multitude of possible structures that colloid particles can form, however, makes experimental study of all possible variations infeasible. Alternatively, theory and computer simulation can be used to identify the structures of interest and guide the discovery of advanced materials in the

laboratory. To do this we need to be able to predict how the kinetics, structure and thermodynamics of the assembly process is affected by (1) particle size and concentration, (2) particle size ratio (for mixtures), (3) electric field strength, (4) dipolar interaction strength and location within the particle, (5) temperature, and (6) the nature, size and ionic strength of solvent and of solutes.

We began by examining a single-component system of dipolar colloid particles with permanent dipole moments immersed in a high-dielectric solvent. [18] Particles were modeled as hard spheres with two oppositely charged small spheres embedded in them. Discontinuous molecular dynamics simulation was used to explore the self-assembly, structure, crystallization and/or gelation of this system. The resulting phase diagram in the inverse temperature (essentially dipole moment/ temperature) – packing fraction plane is shown in Figure 6. Several types of phases are found in our simulations: ordered phases including face centered cubic (FCC), hexagonal close packing (HCP) and body centered tetragonal (BCT) at high packing fractions, and fluid, string-fluid and gel phases at low packing fractions. A series of snapshots of the system as temperature decreases (or equivalently dipole moment increases is shown in Figure 7.

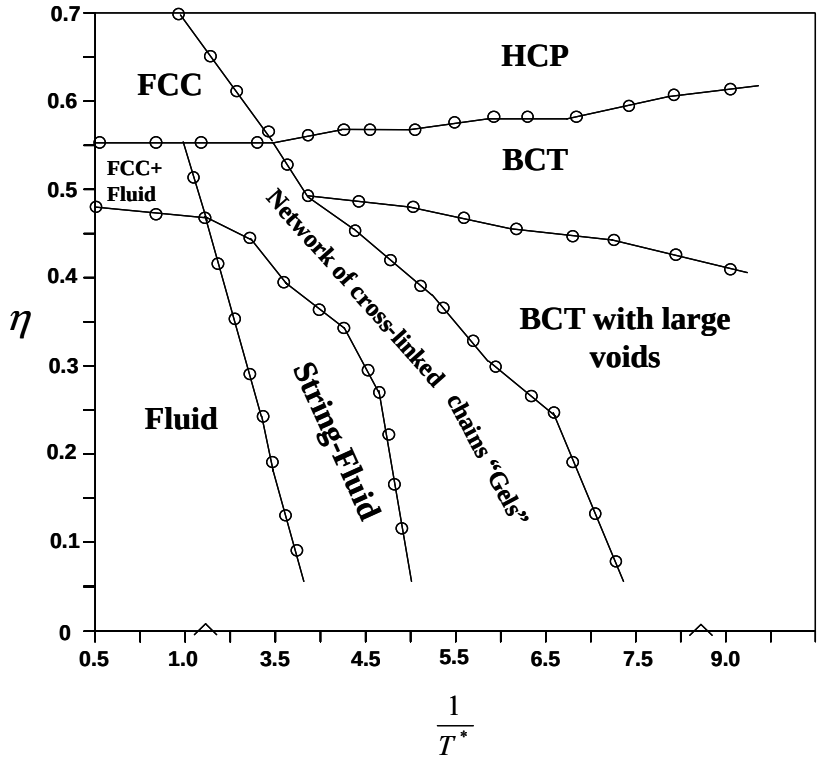

Figure 6: Phase diagram for dipolar colloid particles in the packing fraction (η) – inverse temperature ($1/T^*$) plane. [18]

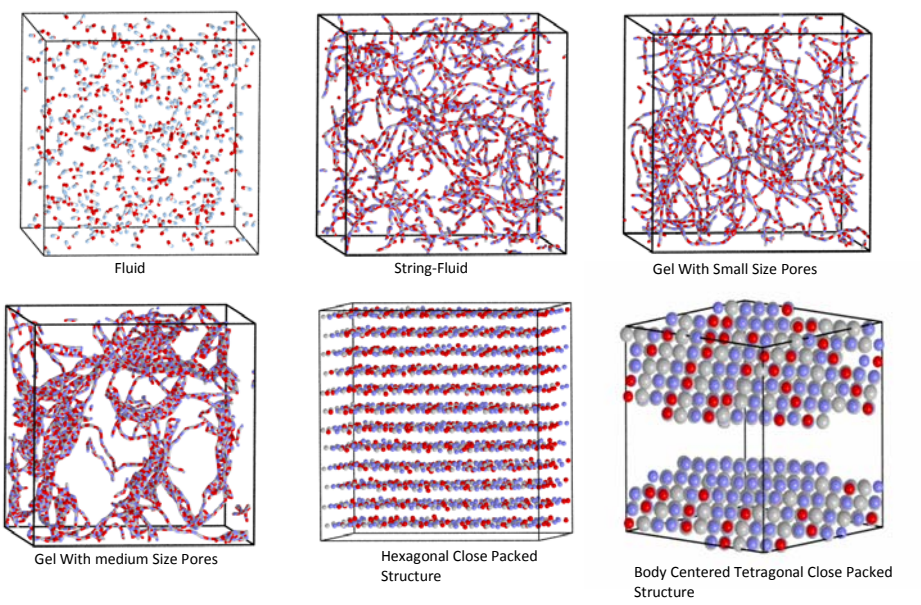

Figure 7 Series of snapshots showing the types of phases encountered as the temperature is reduced, or equivalently the dipole moment is increased . [18]

A novel feature of the phase diagram is the appearance of a percolated gel phase at intermediate temperatures and nearly all particle volume fractions. The high propensity of the dipolar particles to assemble into a network even at very low volume fractions can be attributed to the formation of chains by the particles. A further important aspect of the gelation process is the coarsening of the gel into thicker strands separated by large pores at low temperatures. This implies that the porosity, permeability and mechanical stability of dipolar self-assembled particulate materials can be controlled by tuning the interactions and temperature. Our results help establish, for example, optimal conditions for making sensitive responsive gels using dipolar colloid particles. The particles that we simulate could be used in rapidly-settling gels of low particle volume fractions or in dipolar crystals, which are more robust than crystals formed by uniform spheres. The high sensitivity of dipolar interactions to the ionic concentration in dispersing media means that gels and crystals thus created would be highly responsive to changes in salt, pH, or concentration of ionic adsorbing species. This could allow the systems to be gelled and un-gelled by adding a small volume of acidic, basic, salt or surfactant solution. A variety of other environmentally-sensitive smart materials could be fabricated from such structure-forming suspensions and can be simulated by the procedures presented here.

We next extended this study to a binary mixture of dipolar colloids, differing in size and dipole moment.[20] Phase diagrams for equimolar mixtures of dipolar colloid particles at different diameter ratios and different dipole moment ratios were calculated and plotted in the temperature-volume fraction plane. As was the case for our single component systems several types of phases were found in our simulations: ordered phases including face centered cubic (FCC), hexagonal close packing (HCP) and body centered tetragonal (BCT) at high volume fractions, and fluid, string-fluid and gel phases at low volume fractions. However for certain values of the species diameter ratio (σ_a / σ_b) and ratio of the dipole moments (μ_a / μ_b) , we also found regions of coexistence of ordered phases including $FCC_a + FCC_b$, $FCC_a + HCP_b$, $HCP_a + HCP_b$, $BCT_a + BCT_b$, $BCT_a + BCT_b$ + large voids. Here a and b denote the two species. A phase

diagram for the system with $\sigma_a = \sigma_b$, and $\mu_a = 0.5\ \mu_b$ is shown in Figure 8. Even more interesting was the appearance of a bicontinuous gel phase consisting of network of interpenetrating chains formed by particles with high dipole moment (species b) and chains formed by particles with low dipole moment (species a). Such materials might have distinctive rheological properties such as multiple yield stresses and multiple melting temperatures. The porosity, permeability and mechanical stability of dipolar self-assembled particulate materials can be controlled by tuning the interactions and temperature. A variety of other stimuli-responsive advanced materials could be fabricated from such structure-forming suspensions.

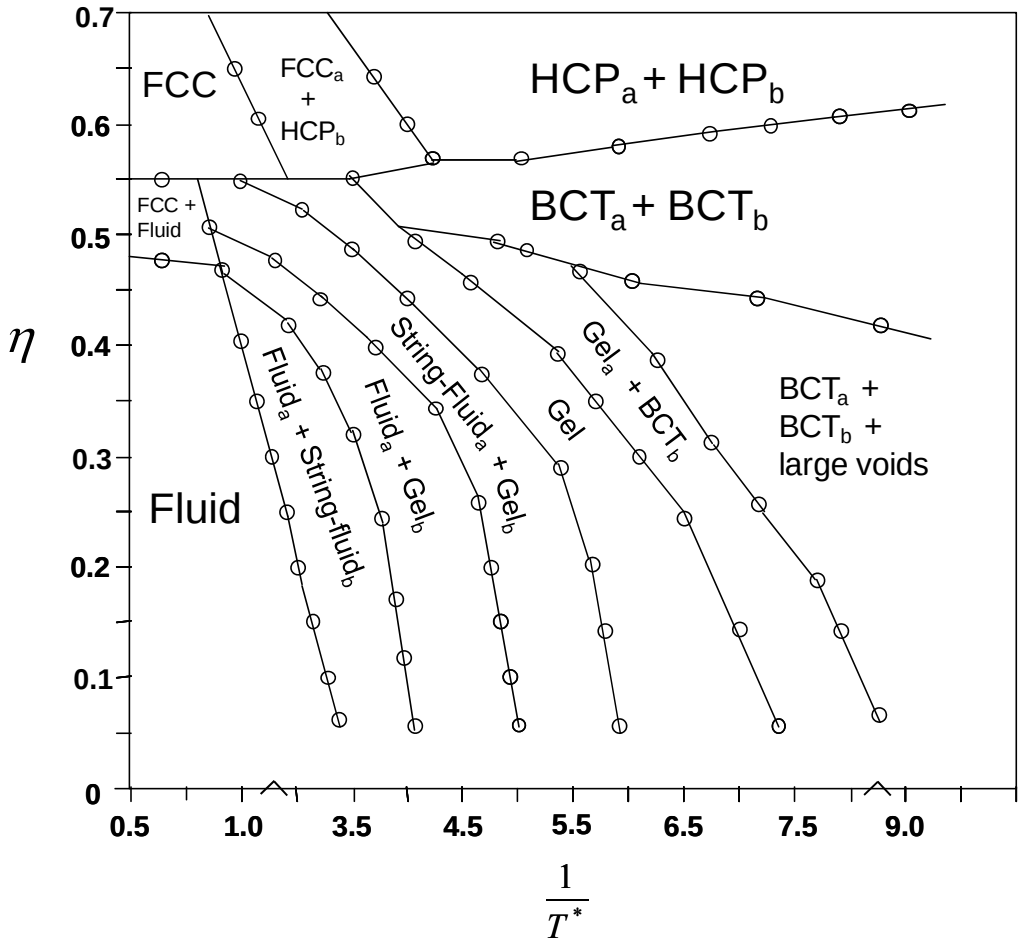

Figure 8: Phase diagram for equimolar binary ($\sigma_a / \sigma_b = 1.0,\ \mu_a / \mu_b = 0.5$) system of dipolar colloid particles in the volume fraction (ϕ) – inverse temperature ($1/T^*$)

plane.

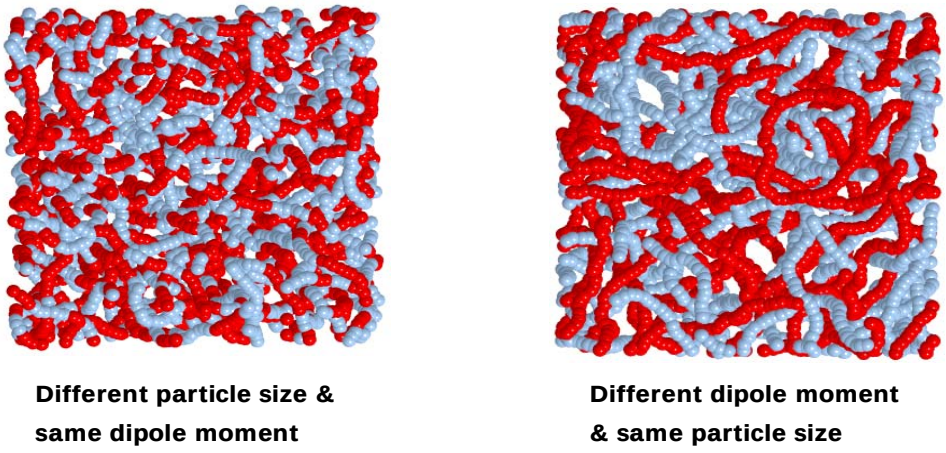

Figure 9. Snapshots of binary mixture of dipolar colloid particles showing percolated network of cross-linked chains (gel) at (a) $\sigma_a / \sigma_b = 0.85, \mu_a / \mu_b = 1.0$. (b) $\sigma_a / \sigma_b = 1.0, \mu_a / \mu_b = 0.5$

Another exciting aspect of these phase diagrams was the appearance of co-crystals of large and small dipolar colloid particles at $\sigma_a / \sigma_b = 0.414$ and μ_a / μ_b =1. These results predict the optimal conditions for making co-crystals which may be the route to the formation of high quality colloidal arrays for photonic and optoelectronic applications.

(5) Mechanically-Assisted Monolayers (MAMs)

Self assembled monolayers (SAMs) are used in a variety of applications including corrosion inhibition, lubrication, flat panel displays and smart windows. Due to this wide array of uses, the ability to "tune" the monolayer's surface characteristics is of vital importance. Although SAMs allow for some adjustment of surface characteristics, their range is limited due to the relatively low surface density of the grafting sites and the accompanying defects that allow penetration of liquids into the monolayer. Mechanically-assisted monolayers (MAMs), which were invented by our colleague Professor Jan Genzer, can rectify the problems associated with low grafting-site surface densities by reaching higher surface coverage than those achievable solely through self-assembly. MAMs are constructed by end-grafting polymer molecules onto a mechanically stretched surface and then releasing the stretch, thereby compressing the polymer brush into a highly dense and highly ordered layer. To this point, all of the research in the area of mechanically-assisted monolayers has been experimental. Thus, at the molecular level, the MAMs formation process and the system characteristics which affect brush formation are unclear.

The project's objective was to improve our understanding of the processes by which mechanically-assisted monolayers form and, by doing so, enable the creation of materials with superior long-lasting barrier properties and tunable characteristics. We simulated the formation of MAMs using discontinuous molecular dynamics (DMD). The MAMs brush is modeled as a system of polymers grafted to a surface. We start at an initial low surface density and then perform Monte Carlo compression attempts to reach higher surface densities; the rate of compression can be correlated to the release rate for MAMs in experiment. One example of simulating this process is shown below in Figure 1 which shows snapshots of a system of fifty 50mers compressed from a low initial density = 0.01 monomers/area, to a final surface density = 0.500.

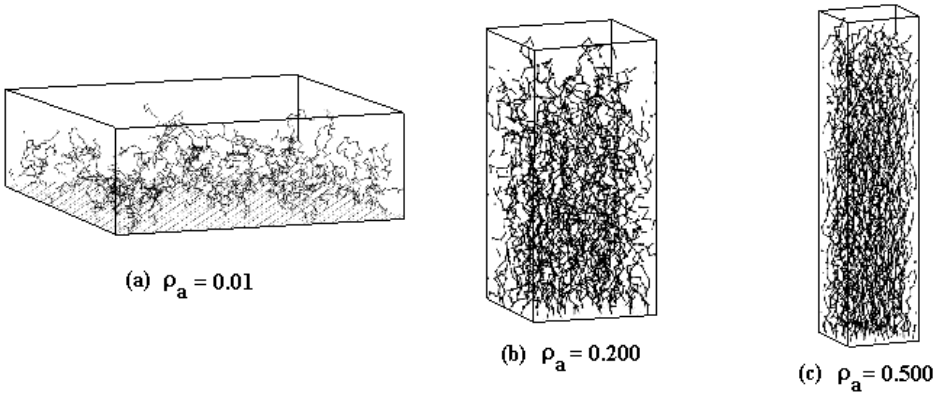

Figure 10: A system consisting of 50 polymers of 50 monomers at an initial surface density of 0.01 monomers per area (a). It is then compressed every 500th collision to surface density 0.200 (b) and, finally to 0.500 (c).

We began by simulating the formation of mechanically assisted monolayers in good solvent. [19] Polymers of chain lengths 5 to 100 were end-grafted to surfaces at low density and then compressed laterally at varying rates. The polymer molecules were modeled as freely jointed hard chains; this is equivalent to good solvent conditions since the monomers feel no long-range attraction to one another. Data for brush thickness and end-monomer density were collected as a function of surface density. We found that brush thickness could be controlled by judicious choice of the compression rate. Defects in the brush layer were dependent on chain length; it was shown that quick compression for relatively short chains allowed the layer no time to relax into coil form. Quick compression on long chain systems led to entanglement in the brush layer since the longer-chains were not afforded the long relaxation time required to form a fully-relaxed brush. Hysteresis effects were examined by allowing the brush to relax to a lower surface density. Higher surface compression/relaxation rates led to an increase in disparity between the brush thickness found during the compression and brush thickness found during relaxation. This disparity was due to inadequate equilibration times. Lastly, results from non-uniform compression in good solvent showed negligible effects on monolayer height and structure.

Although we neglected the effect of solvent quality in the work described above, solvent quality is known to play an important role in polymer behavior and likely in the formation of MAMs and polymer brushes. Quick compression of brushes created via the MAMS process at poor solvent qualities could limit the extension of the polymers away from the substrate, preventing the monolayer from forming a dense, impenetrable brush. This might be the source of the substrate buckling observed experimentally during quick MAMS compressions.

In an attempt to mimic the formation of MAMs in a poor or less than ideal solvent we performed discontinuous molecular dynamics simulations of the compression of systems of polymers modeled as chains of square-well monomers. [21] Polymers of chain lengths 20, 50 and 100 were initially grafted to a hard surface at low density and allowed to equilibrate. These chains

were then compressed at varying rates to high surface density to study the effects of chain length and compression rate on brush thickness. We found that brush thickness could be directly controlled by adjusting the system reduced temperature (which indirectly controls solvent quality) and surface compression rate. Brushes formed at temperatures below the theta temperature (T_θ) and/or at low surface density showed significant brush degradation (gaps in polymer layer coverage and thin brushes). Brushes formed at temperatures above T_θ were relatively thick and nicely ordered; they could reach higher surface densities than brushes formed at low temperatures. We found that fast compression led to end-monomer and chain trapping. Last, we showed that for every compression rate, there exists a surface density, beyond which further compression attempts are not likely to be successful. From this, we infer that the best plan for MAM fabrication is to systematically decrease the compression rate as surface density increases.

Student Training

The following Ph. D. recipients were trained during this project. The titles of their theses and current affiliations are also given.

1. Brian Attwood, Ph.D., '03, "Monte Carlo Simulation of Solid Fluid Phase Equilibria in Binary and Ternary Mixtures", now at the EPA.

2. Andrew Schultz,Ph.D., '04, "Modeling & Computer Simulation of Block Copolymer Nanoparticle Composites", now a research assistant professor at the University of Buffalo

3. Aysa L. Galbraith "Solid-Liquid Equilibrium for Chiral Drug Separations", now an instructor at NorthWest Arkansas Community College.

4. Arthi Jayaraman, Ph.D., '05, "Design of Pattern Recognition Surfaces", University of Colorado, Assistant Professor.

Two more DOE-supported students, Amit Goyal and L. Anderson Strickland will defend their Ph.D. theses this winter.

Papers Published

1. M. H. Lamm and C. K. Hall, "The Effect of Pressure on the Complete Phase Behavior of Binary Mixtures, AIChE J. **50**, 215 (2004)
2. A. J. Schultz, C. K. Hall and J. Genzer, "Box Length Search Algorithm for Systems Containing Periodic Structures," J. Chem. Phys. **120**, 2049 (2004).
3. B. C. Attwood and C. K. Hall, "Effect of the Solid Phase on the Global Phase Behavior of Binary Lennard Jones Mixtures," AIChE J. **50**, 1948 (2004).
4. A. Van 'Thof, S. W. DeLeeuw, C. K. Hall and C. J. Peters, "Molecular Simulation of Binary Vapor-Liquid Equilibria with Components Differing Largely in Volatility," Molec. Phys. **102**, 301 (2004).
5. J. A. McCormick and C. K. Hall, "The Dynamics of Single Chains Within a Polymer Melt," J. Chem. Phys. **122**, 114902 (2005).
6. A. J. Schultz, C.K. Hall and J. Genzer, "Computer Simulations of Block Copolymer Nanoparticle Composites," Macromolecules **38**,3007 (2005).

7. A Jayaraman, C. K. Hall and J. Genzer, "Designing Pattern Recognition Surfaces for Selective Adsorption of Copolymer Sequences Using Lattice Monte Carlo Simulation, Phys Rev Lett. **94,** 078103 (2005)
8. A. Striolo, A. Jayaraman, J. Genzer and C.K. Hall, "Adsorption of Comb Copolymers on Weakly Attractive Solid Surfaces, J. Chem Phys. . 123, 064710 (2005).
9. A. Jayaraman, J. Genzer and C.K. Hall, "Computer Simulation Study of Pattern Transfer in AB Diblock Copolymer Films Adsorbed on Heterogeneous Surface", J. Chem Phys. 123, 124702 (2005).
10. A. L Galbraith and C. K. Hall, Vapor-liquid phase equilibria for mixtures containing diatomic Lennard-Jones molecules, Fluid Phase Equilibria, **241**,175(2006)
11. A. J. Schultz, C.K. Hall and J. Genzer, "Obtaining Concentration Profiles from Computer Simulation Structure Factors," Macromolecules **40**, 2629-2632 (2007).
12. A. L. Galbraith and C. K. Hall, "Solid-Liquid Phase Equilibria for Mixtures Containing Diatomic Lennard Jones Molecules," Fluid Phase Equilibria , **262**,1 (2007).
13. A. Jayaraman, C. K. Hall and J. Genzer, "Computer Simulation Study of Molecular Recognition in Model DNA Microarrays," Biophys J, **91**, 2227 (2006).
14. A. J. Schultz, C.K. Hall and J. Genzer, "Obtaining Concentration Profiles from Computer Simulation Structure Factors," Macromolecules **40**, 2629-2632 (2007).
15. A. Jayaraman ,E. E. Santiso C.K. Hall and J. Genzer, "Theoretical Study of Kinetics of Hybridization in DNA Microarrays, Phys Rev E **76**, 011915 (2007) .
16 A. Jayaraman ,C.K. Hall and J. Genzer, "Computer Simulation Study of Probe-Target Hybridization in Model DNA Microarrays : Effect of Probe Surface Density and Target Concentration," J. Chem. Phys. **127**, 144912 (2007).
17 B. C. Attwood and C. K. Hall, Solid-Liquid Phase Behavior of Ternary Mixtures, AIChE J. published on-line May 22, 2008.
18 A Goyal, C. K Hall and O. Velev, "Phase diagram for stimulus-responsive materials containing dipolar colloidal particles," Phys. Rev E **77**, 031401 (2008).
19 L.A. Strickland, C. K. Hall and J. Genzer, "Simulation of Mechanically-Assembled Monolayers and Polymers in Good Solvent Using Discontinuous Molecular Dynamics", Macromolecules,**41** ,6573 (2008).
20. A. Goyal, C.K. Hall and O. Velev, **"**Computer Simulation of Aggregation in Binary System of Dipolar Colloid Particles," manuscript in preparation.
21. L. L.A. Strickland, C. K. Hall and J. Genzer," Simulation of Mechanically-Assembled Monolayers in Varying Solvent Using Discontinuous Molecular Dynamics," manuscript in preparation.